# THE EFFECT AND CONTRIBUTION OF WIND GENERATED ROTATION ON OUTLET TEMPERATURE AND HEAT GAIN OF LS-2 PARABOLIC TROUGH SOLAR COLLECTOR

by

***Omid Karimi SADAGHIYANI [a]*, Seyed Mehdi PESTEEI [b], and Iraj MIRZAE [b]***

[a] Department of Mechanical Engineering, Islamic Azad University, Khoy branch, Khoy, Iran
[b] Department of Mechanical Engineering, Urmia University, Urmia, Iran

Original scientific paper
DOI: 10.2298/TSCI110613123S

*The Monte Carlo ray tracing method is applied and coupled with finite volume numerical methods to study effect of rotation on outlet temperature and heat gain of LS-2 parabolic trough concentrator. Based on effect of sun-shape, curve of mirror and use of Monte Carlo ray tracing, heat flux distribution around of inner wall of evacuated tube is calculated. After calculation of heat flux, the geometry of LS-2 Luz collector is created and finite volume method is applied to simulate. To validate these numerical solving models, the obtained results were compared with Dudley et al. test results for irrotational cases and with Ball's results. In this work, according to the structure of mentioned collector, we use plug as a flow restriction. In the rotational case studies, the inner wall rotates with different angular speeds. We compare results of rotational collector with irrotational. Also for these two main states, the location of plug changed then outlet temperature and heat gain of collector are studied. The results show that rotation have positive role on heat transfer processing and the rotational plug in bottom half of tube have better effectual than upper half of tube. Also the contribution of rotation is calculated in the all of case studies. Working fluid of these study is one of the oil derivatives namely Syltherm-800. The power of wind can be used to rotate tube of collector.*

Key words: *parabolic trough collector, LS-2 collector, contribution of rotation, outlet temperature*

## Introduction

Since the 1970, many simulations and experiments on solar systems were published, especially on the parabolic trough concentrator (PTC). The purpose of some of them was reduction on costs and increasing of performance by new designs, others had been applied to improving the reliability of receiver tubes, and selective coating performance [1, 2]. After these developments of experiments on solar systems, the numerical studies were performed widely [3]. Most of these studies are 1-D and based on the first law of thermodynamics [4, 5] or based on second law [6, 7]. 2-D efficiency analysis models were developed recently [8, 9].

As early as in 1977, analytical modeling of PTC was used by Evans [10], and Harris and Duff [11]. Then, Jeter [12, 13] calculated a first integral of the concentrated radiant heat flux density for linear parabolic collectors. Sundia National Research Laboratory (SNRL) specified the thermal loss and collector efficiency of the LS-2 Solar Energy Generating Systems (SEGS) trough collector Dudley *et al.* [4]. An optical model of the PTC has been improved by Heinzel *et al.* [3].

* Corresponding author; e-mail: st_o.sadaghiyani@urmia.ac.ir

The solar rays after reflecting from parabolic surface focus on outer wall of absorber tube. In this work, heat flux distribution around of tube is calculated by the in-house developed code based on the Monte Carlo ray tracing (MCRT) method [14]. Consider that the sun rays were assumed non-parallel. 3-dimensional finite volume numerical modeling applied and coupled with MCRT method to simulate LS-2 solar collector that tested at SNRL. In this work, we try to study effect of rotation on heat transfer characteristics such as outlet temperature and heat gain compared with irrotational walls. In these case studies the inner wall (plug) of collector rotated respectively. The power source of rotation is wind force.

## Model description

To be able to validate the MCRT method for influenceof flux distribution that is function of structural and geometrical parameters, results are compared with Jeter's analytical results. Also in order to validate finite volume numerical methods, results are compared with Dudley *et al*. results [4] and Ball *et al.* [15]. In tab. 1 the structural properties of mentioned collector are:

**Table 1. The list of LS-2 collector structural properties**

| LS-2 PTC (as tested as SNRL) | |
|---|---|
| Manufacturer | Luz industrial, Israel |
| Operating temperature | 100-400 °C |
| Module size | 7.8 m × 5 m |
| Rim angle | 70 degrees |
| Reflector | 12 thermally sagged glass panel |
| Aperture area | 39.2 $m^2$ |
| Focal length | 1.84 m |
| Concentration ratio | 22.74 |
| Receiver | Evacuated tube, metal bellows at each end |
| Absorber diameter | 70 mm |
| Glass cover | |
| Diameter | 115 mm |
| Transmittance | 0.95 |
| Absorber surface | Cermet selective surface |
| Absorptance | 0.96 |
| Absorber tube inner diameter | 66 mm |
| Absorber tube outer diameter | 70 m |

## Governing equations

As the test conditions, the fluid flow is turbulence and in steady state condition. So the governing equations for continuity, momentum, standard $k$-$\varepsilon$ and energy are fundamental equations for turbulence models can be written as:

– *continuity*

$$\frac{\partial}{\partial x_i}(\rho u_i) = 0 \tag{1}$$

– *momentum equation*

$$\frac{\partial}{\partial x_i}(\rho u_i u_j) = -\frac{\partial p}{\partial x_i} + \frac{\partial}{\partial x_i}\left[(\mu_t + \mu)\left(\frac{\partial u_i}{\partial x_j} + \frac{\partial u_j}{\partial x_i}\right) - \frac{2}{3}(\mu_t + \mu)\frac{\partial u_i}{\partial x_i}\delta_{ij}\right] + \rho g_i \tag{2}$$

– *energy equation*

$$\frac{\partial}{\partial x_i}(\rho u_i T) = \frac{\partial}{\partial x_i}\left[\left(\frac{\mu}{\mathrm{Pr}} + \frac{\mu_\mathrm{t}}{\sigma_\mathrm{T}}\right)\frac{\partial T}{\partial x_i}\right] + S_R \tag{3}$$

– $k$ equation

$$\frac{\partial}{\partial x_i}(\rho u_i k) = \frac{\partial}{\partial x_i}\left[\left(\mu + \frac{\mu_\mathrm{t}}{\sigma_\mathrm{k}}\right)\frac{\partial k}{\partial x_i}\right] + G_\mathrm{k} - \rho\varepsilon \tag{4}$$

– $\varepsilon$ equation

$$\frac{\partial}{\partial x_i}(\rho u_i \varepsilon) = \frac{\partial}{\partial x_i}\left[\left(\mu + \frac{\mu_t}{\sigma_\varepsilon}\right)\frac{\partial \varepsilon}{\partial x_i}\right] + \frac{\varepsilon}{k}(c_1 G_\mathrm{k} - c_2\rho\varepsilon) \tag{5}$$

where the turbulence viscosity and the production rate are expressed by:

$$\mu_\mathrm{t} = c_\mu \rho \frac{k^2}{s}$$
$$G_k = \mu_t \frac{\partial u_i}{\partial x_j}\left(\frac{\partial u_i}{\partial x_j} + \frac{\partial u_j}{\partial x_i}\right) \tag{6}$$

The standard constants used: $c_\mu = 0.09$, $c_1 = 1.44$, $c_2 = 1.92$, $\sigma_\mathrm{k} = 1.0$, $\sigma_\varepsilon = 1.3$, and $\sigma_\mathrm{T} = 0.85$.

**Boundary conditions**

The boundary conditions that are applied to the inlet and outlet of collector tube:

– *for inlet*

$$\dot{m}_\mathrm{x} = 0.6782 \text{ kg/s}, \quad \dot{m}_\mathrm{y} = \dot{m}_\mathrm{z} = 0 \text{ kg/s}, \quad T_{in} = 375.5 \text{ K}$$

$$k_\mathrm{in} = 0.01\cdot(1/2)u_{in}^2, \quad \varepsilon_\mathrm{in} = \varepsilon_\mathrm{in} = \frac{c_\mu \rho(t)}{\mu_t} k_{in}^2, \text{ where } c_\mu = 0.09, \text{ and } \mu_\mathrm{t} = 100 \text{ [16]}$$

Also mass flow inlet boundary condition has been applied.

– *for outlet*

The fully-developed assumption and outflow boundary conditions are considered.

The amount of direct normal incident that used to simulated Sun rays is 933 W/m$^2$. The heat transfer fluid (HTF) is Syltherm-800 liquid oil that its properties are functions of temperature:

$$c_p = 0.00178T + 1.107798 \text{ kJ/kgK} \tag{7}$$

$$\rho = -0.4153495T + 1105.702 \text{ kg/m} \tag{8}$$

$$k = -5.753496\cdot10^{-10}T^2 - 1.875266\cdot10^{-4}T + 0.1900210 \text{ W/mK} \tag{9}$$

$$\mu = 6.672\cdot10^{-7}T^4 - 1.566\cdot10^{-3}T^3 + 1.388T^2 - 0.05541T + 8.487\cdot10^4 \text{ μPa·s} \tag{10}$$

The substance of solid material is stainless steel-304 with conductivity 54 W/mK.

According to fig. 1, the thermal boundary condition around of tube is a function of $\theta$ in polar co-ordination system that two conditions are calculated. The sun rays are converged or assumed parallel. In this article, the heat flux of converged rays is applied and used to simulated LS-2 collector. Consider that the angle of convergence is 16 degree.

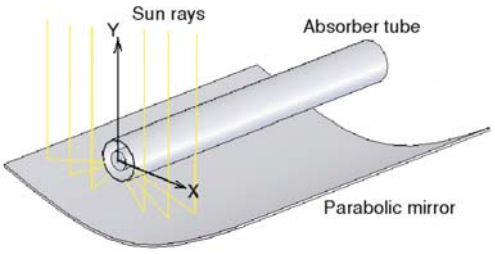


**Figure 1. shows the parabolic trough collector and Sun rays schematically**

The density of heat flux around the absorber tube of parabolic trough collectors is important for the maximizing of optical performance and explained heat transfer processing widely [17]. It is illustrated in the form of the local concentration ratio (LCR) in fig. 3, which is function of $\theta$. The flowchart of MCRT simulation is presented in fig. 2. Based on MCRT method, MATLAB software is applied. Of course, to reach to heat flux distribution, it is necessary to

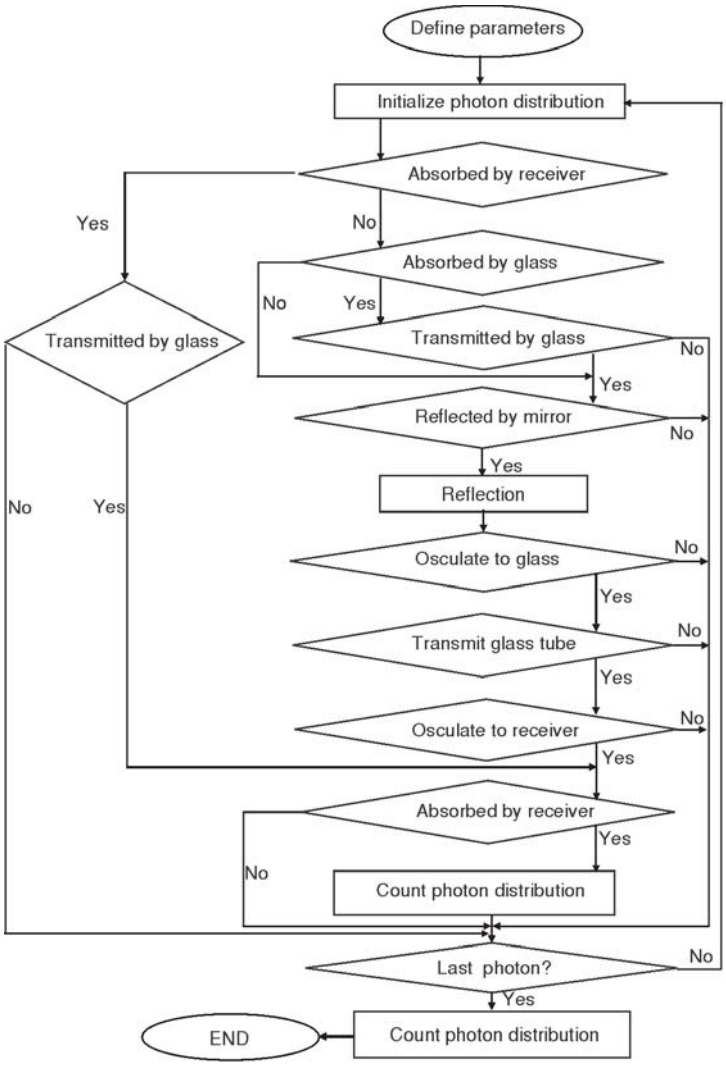


**Figure 2. The flowchart of MCRT in MATLAB software**

multiply LCR by the value of the incident irraiance.

## Numerical methods

Several mesh systems are generated to test independent of grids. These grid systems contain ($N_c$ = 70, $N_z$ = = 340), ($N_c$ = 70, $N_z$ = 4300), ($N_c$ = 70, $N_z$ = 500) and ($N_c$ = 90, $N_z$ = 340). Obtained results showed good agreement together.

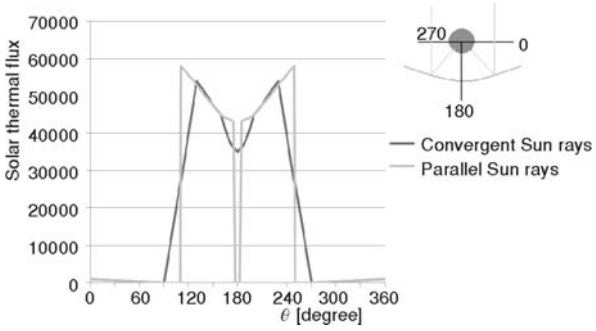


**Figure 3. Schematics of heat flux distribution around receiver tube**

The fundamental equations were discretized by the finite volume method [18] and the convective terms in momentum and energy equations were discretized with the second upwind scheme. The SIMPLE algorithm was applied to coupling between velocity and pressure [19]. Consider that the convergence criterion for the velocity and energy was the maximum residual of the first ten iterations was less than $10^{-5}$ and $10^{-7}$, respectively. The results of numerical simulation compare with Dudley *et al*. [3] experimental results.

Consider to tab. 2 that conditions of environment and comparing of numerical and experimental results together are presented.

**Table 2. The comparison between experimental data and numerical results in order to validation**

| Case study | Direct normal incident [Wm$^{-2}$] | Mass flow rate [Lmin$^{-1}$] | Air temperature [°C] | Inlet temperature [°C] | Outlet temperature [°C] exp. | Outlet temperature [°C] num. | $\eta$ Efficiency num. [%] |
|---|---|---|---|---|---|---|---|
| 1 | 933.7 | 47.7 | 21.2 | 102.2 | 124.0 | 124.2 | 72.07 |
| 2 | 982.3 | 49.1 | 24.3 | 197.5 | 219.5 | 220.4 | 71 |
| 3 | 909.5 | 54.7 | 26.2 | 250.7 | 269.4 | 271 | 70.5 |
| 4 | 937.9 | 55.5 | 28.8 | 297.8 | 316.9 | 318 | 68.5 |

So, the solving method is validated and used for others studies that we change angular speeds of outer wall or plug rotation with several position of plug. The working fluid of these studies is Syltherm-800 and the kind of tube and plug is stainless steel 304. The applied angular speeds that have been used in this work, are 10, 20, and 50 rad/s (fig. 4). For preparation of these speeds we can use from little wind tools. If we use over driver gear-boxes wich change low angular speeds to high and uniform angular speeds then, the power of wind is used on heat transfer processing. The x-axes in diagrams are non-dimensional displacement of plug from tube center that is defined as:

Non-dimensional displacement = $2d_p/(D_i - D_p)$

Results of these case studies are given as follows. Figure 5 shows a diagram of outlet temperature for $D_p$ = 30 mm with angular speeds = 10, 20, and 50 rad/s comparing with irrotational case.

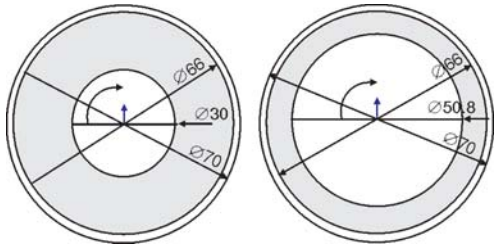


**Figure 4. The cross-sections of absorber tubes and their plugs (30 and 50.8 mm, respectively)**

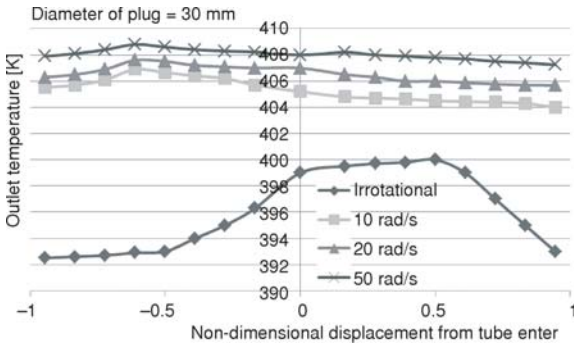


**Figure 5. Effect of rotation and position of plug on outlet temperature (diameter of plug = 30 mm)**

Obviously, at irrotational case, it is found that, for non-dimensional displacement = 0.5, maximum outlet temperature can be reached, but at rotational cases, this maximum temperature locate at non-dimensional displacement = –0.5. Other conclusion that we obtain, it is that for high angular speeds, the displacement of plug have low effect rather than low angular speeds. These results are so similar to other diameters results, such as 50.8. In this figure, regard all of diagrams separately specially the variation between maximum and minimum outlet temperature points. It is concluded that, on high angular speeds, the impressibility of outlet temperature from location is low and if the angular speed increases likewise, the trend of diagram will be constant function. The variation between each of rotational cases with irrotational, show the effect of rotation on heat transfer processing. These influences are shown in diagram of plug that its diameter is 50.8 mm.

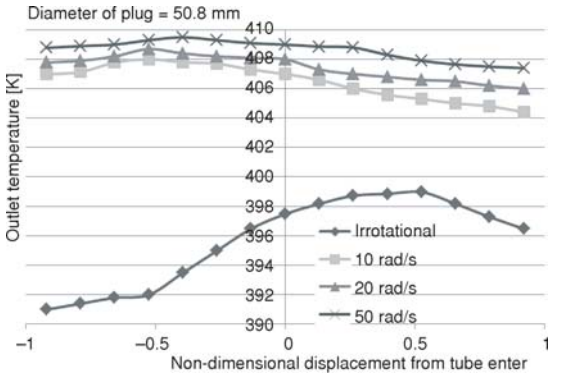


**Figure 6. Effect of rotation and position of plug on outlet temperature (diameter of plug = 50.8 mm)**

Figure 6 shows a diagram of outlet temperature for $D_p$ = 50.8 mm with angular speeds =10, 20, and 50 rad/s comparing with irrotational case:

In the other study, effect of diameter on heat transfer is analyzed, so if diameter of plug increases, collecting of solar energy will be improved. Figure 7 shows the effect of diameter of plug on outlet temperature. In this figure, at the left of irrotational case, the trend of diagram is decreasing, because, in the low diameters, the natural convection is very effective role on good mixing of flow. But on the rotational plugs effects of natural convection is negligible. Considering this convergence of diagrams at right hand, it is understood, increasing the angular speed at low diameters is more effective than high diameters.

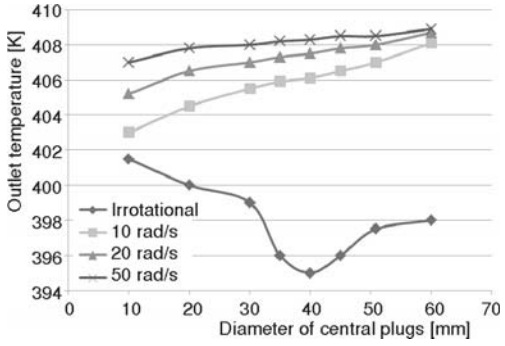


**Figure 7. Effect of diameter on outlet temperature for central plugs**

## Thermal efficiency and amount of heat gain

The useful heat gain by the parabolic trough collector exposed to solar radiation with measured values of inlet and outlet temperatures and mass flow rate ($\dot{m}$) and specific heat of fluid ($c_p$) is defined as:

$$Q_{\mathrm{u}} = \dot{m} c_p (T_{\mathrm{o}} - T_i) \tag{11}$$

where the efficiency of the collector is calculated by:

$$\eta_{\mathrm{th}} = \frac{Q_{\mathrm{u}}}{A_{\mathrm{c}} I} \tag{12}$$

Here $A_{\mathrm{c}}$ is the area of the collector and $I$ – the solar radiation incident on the collector mirror. If the power of wind acts on the solar systems via mill then the relation of efficiency is changed as:

$$\eta_{\mathrm{th}} = \frac{Q_{\mathrm{u}}}{A_{\mathrm{c}} I + \text{wind energy}} \tag{13}$$

This formula needs the calculated amount of wind energy. But for good comparison with irrotational case, we present a relation:

$$\text{Percent of heat gain toward approached solar heat} = Q_{\mathrm{u}}/A_{\mathrm{c}} I \tag{14}$$

The effect of rotation and its angular speeds and location on the heat gain were calculated, the following diagrams show amounts of outflow temperature and heat gain toward approached solar heat, after applying these changes for $D_{\mathrm{p}}$ = 30 mm and 50.8 mm, respectively (figs. 8 and 9).

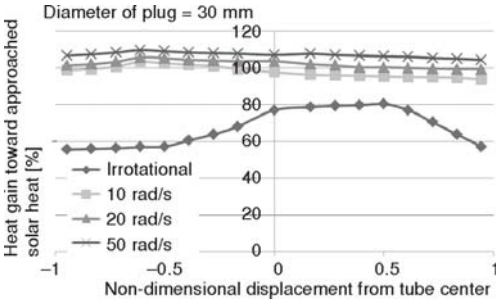


**Figure 8. Comparison between rotational inner wall with various angular speeds and irrotational walls**

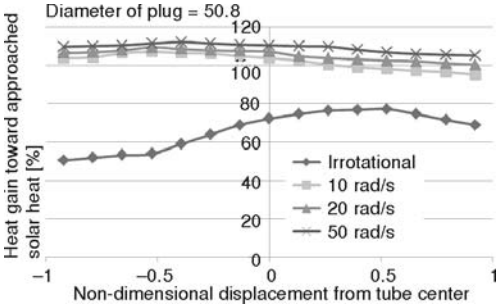


**Figure 9. Diagram of heat gain toward approached solar heat**

Obviously, the variation between maximum and minimum points for each of diagrams show that on high angular speeds, the impressibility of energy collecting and heat gain from plug location is low and if the angular speed likewise increase the trend of diagram will be constant function. As the maximum variation happen in irrotational case study. The variations between each of rotational cases diagrams with irrotational diagram, show the effect of rotation on heat transfer processing. These influences are shown in diagram of fig. 9 that its diameter is 50.8mm.

We used rotated central plugs with several diameters. According to fig. 10 it is concluded

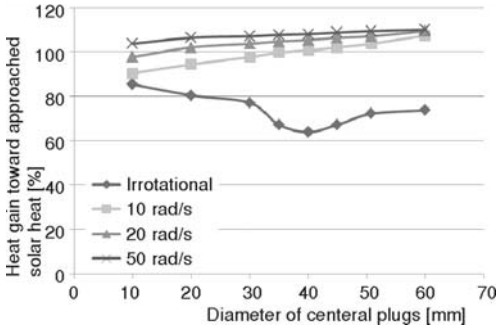


**Figure 10. Diagram of heat gain toward approached solar heat for central plugs**

that, if the diameter of plug increase, effect of angular speed will be pale, unlike irrotational case.

## Contribution of rotation on heat transfer processing

We present one relation that expresses contribution of rotation on heat transfer processing, because both of the solar energy and the wind energy contribute on heat transfer processing. Solar energy via heat flux generation and wind energy via rotation [20]. The rotation has two effects on process: firstly, mixing, and so increasing of Nusselt number, secondly, heat generation due to friction. So we try to know effect of rotation and its contribution on heating of liquid oil.

$$\text{Contribution of rotation on heat transfer processing} = \frac{Q_{\text{rot}} - Q_{\text{irr}}}{Q_{\text{rot}}} \tag{15}$$

$$\text{Consider that each of } Q_{\text{rot}} \text{ and } Q_{\text{irr}} \text{ are calculated via } \mathrm{Q} = \dot{m} c_p (T_{\text{o}} - T_{\text{i}}). \tag{16}$$

After calculation the contribution of rotation on heat gain can be reached. These results are shown in figs. 11, 12, and 13.

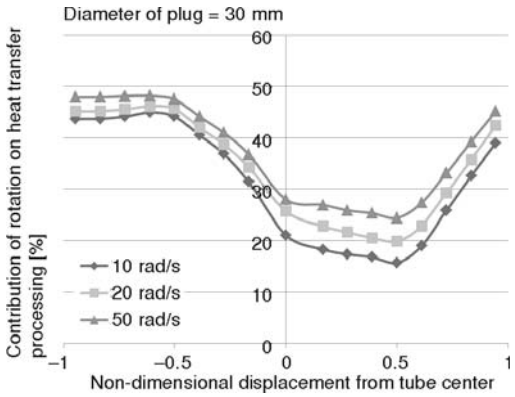


**Figure 11. Contribution of rotation on heat transfer processing for plug with diameter = 30 mm**

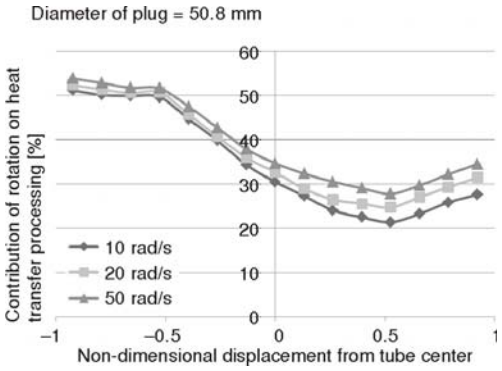


**Figure 12. The contribution of rotation on heat transfer processing for plug with diameter = = 50.8 mm**

Also the contribution of rotation on heat transfer processing for the central plugs with several diameters are calculated in fig. 12 these effects are shown clearly.

## Conclusions

In this work, 3-D analysis of heat transfer characteristics in the evacuated tube is performed by coupling the MCRT and numerical simulation methods. Three parameters selected to change (diameter of plug, location of plug, and angular speeds). The aims of these changes are study of outlet temperature and efficiency of

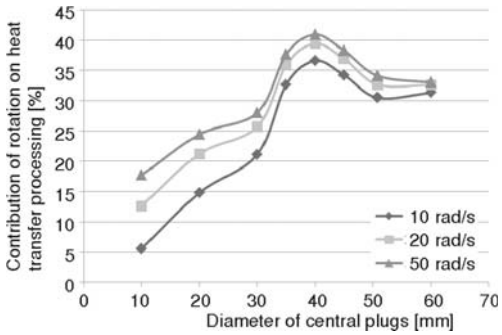


**Figure 13. Contribution of rotation on heat transfer processing for central plugs**

collectors. Notice that likely when the amount of non-dimensional displacement of irrotational plug from tube center = 0.5, then the maximum outlet temperature and efficiency can be reached. Also, for rotational states, the maximum outlet temperature and efficiency located at non-dimensional displacement = –0.5. It is the other conclusion that increasing the angular speed at low diameters is more effective than high diameters. In this work, we studied effect of wind energy in outlet temperature and analyzed contribution of rotation on heat transfer processing at parabolic trough collectors. This study says that if the wind contributes in heat transfer, outlet temperature will be increase 10% until 60%. Also at $D_p = 40$ mm, the contribution of rotation in heat transfer is most.

## Nomenclature

$A_c$ – aperture area
$c_\mu$, $c_1$, $c_2$ – coefficients in the turbulence model
$D$ – diameter, [m]
$I_b$ – direct normal irradiance [$Wm^{-2}$]
$K$ – incident angle modifier
$k$ – thermal conductivity, [$Wm^{-1}K^{-1}$]
$\dot{m}$ – mass flow rate, [$kgs^{-1}$]
$N$ – number of mesh
Pr – Prandtl number
$Q_{irr}$ – heat gain in irrotational state
$Q_{rot}$ – heat gain in rotational state
$Q_u$ – usefull heat gain
$q_{loss}$ – thermal loss [$Wm^{-2}$]
$q_{mass}$ – flow rate [$kgs^{-1}$]
Re – Reynolds number based on tube hydraulic diameter
$S_R$ – additional source term [$Wm^{-3}$]
$T$ – temperature (K)
$\Delta T_{ab}$ – receiver fluid temperature above ambient air temperature [K]
*u, v,w, x, y, z* – velocity components [$ms^{-1}$]
x, y, z – Cartesian co-ordinates

*Greek symbols*

$\varepsilon$ – turbulent dissipation rate or emissivity
$\eta$ – collector efficiency calculated by test data
$\eta'$ – collector efficiency calculated by simulation data
$\kappa$ – thermal conductivity or kinetic energy
$\mu$ – dynamic viscosity [Pa·s]
$\mu_t$ – turbulent viscosity [Pa·s]
$\nu$ – kinematic viscosity [$m^2s^{-1}$]
$\rho$ – density [$kgm^{-3}$]
$\sigma_T$ – turbulent Prandtl number
$\sigma_k$, $\sigma_s$ – turbulent Prandtl numbers for diffusion of $k$ and $\varepsilon$

*Subscripts*

a – ambient
c – circumference
i, j, k – unit vectors at x-, y-, and z-directions
in – inlet parameters
m – mean or average value
o – outlet parameter or outer
p – plug
t – turbulent
th – thermal
z – z-co-ordination system direction

## References

[1] Price, H., *et al*., Advances in Parabolic Trough Solar Power Technology, *J. Solar Energy, 124* (2002), 2, pp. 109-125
[2] Kalogirou, S. A., Solar Thermal Collectors and Applications, *Prog. Energy Combust. Sci., 30* (2004), 3, pp. 231-295
[3] Heinzel, V., Kungle, M. S., Simulation of a Parabolic trough Collector, ISESSolar World Congress, Harare, Zimbabwe, 1995, pp. 1-10
[4] Dudley, V., *et al*., SEGS LS2 Solar Collector – Test Results, Report of Sandia National Laboratories, SANDIA94-1884, Albuquerque, New. M., USA, 1994
[5] Forristall, R., Heat Transfer Analysis and Modeling of a Parabolic trough Solar Receiver Implemented in Engineering Equation Solver, Technical Report, NREL/ TP-550-34169, 2003
[6] Eskin, N., Transient Performance Analysis of Cylindrical Parabolic, *Energy Convers. Manage, 40* (1999), 2, pp. 175-191
[7] Tyagi, S. K., *et al.*, Exergy Analysis and Parametric Study of Concentrating Type Solar Collectors, *International journal of Thermal Science 46* (2007), 12, pp. 1304-1310
[8] Naeeni, N., Yaghoubi, M., Analysis of Wind Flow Around a Parabolic Collector (2) Heat Transfer from Receiver Tube, *Renewable Energy, 32* (2007), 8, pp. 1259-1272

[9] Naeeni, N., Yaghoubi, M., Analysis of Wind Flow Around a Parabolic Collector (1) Fluid Flow, *Renewable Energy, 32* (2007), 11, pp. 1898-1916
[10] Evans, D. L., On the Performance of Cylindrical Parabolic Solar Concentrators with Flat Absorbers, *Solar Energy, 19* (1977), 4, pp. 379-385
[11] Harris, J. A., Duff, W. S., Focal Plane Flux Distribution Produced by Solar Concentrating Reflectors, *Solar Energy, 27* (1981), 5, pp. 403-411
[12] Jeter, S. M., Calculation of the Concentrated Flux Distribution in Parabolic trough Collectors by a Semifinite Formulation, *Solar Energy, 37* (1986), 5, pp. 335-345
[13] Jeter, S. M., Analytical Determination of the Optical Performance of Parabolic trough Collectors from Design Data, *Solar Energy, 39* (1987), 1, pp. 11-21
[14] Xiao, J., *et al*., Simulation for Concentrating Characteristics of Parabolic Solar Collector, Part A: Analysis of Concentrating Characteristics, *Proceedings,* 14thAnnual Symposium of Chinese Society of Engineering Thermophysics, Tianjin, China, 2008
[15] Ball, K. S., *et al.*, An Experimental Study of Heat Transfer in a Vertical Annulus with a Rotating Inner Cylinder, *International Journal of Heat and Mass Transfer, 32* (1989), 8, pp. 1517-1527.
[16] Tao, W. Q., *Numerical Heat Transfer*, 2nd ed, Xi'an Jiaotong University Press, Xi'an, China, 2001
[17] Dudley, V. E.,Workhoven, R. M. Performance Testing of the Solar Kinetics T-700A Solar Collector. Tech. Rep. No.SAND81-0984, SANDIA, Albuquerque, N. Mex., USA, 1982
[18] Odeh,S. D., *et al*., Thermal Analysis of Parabolic trough Solar Collector for Power Generation, *Proceedings,* ANZSES 34th Annual Conference, Darwin, Australia, 1996, pp. 460-467
[19] Shuai, Y., *et al*., Tan, Radiation Performance of Dish Solar Concentrator/Cavity Receiver Systems, *Solar Energy, 82* (2008), 1, pp. 13-21
[20] Romero, M., *et al*., Terrestrial Solar Thermal Power Plants: on the Verge of Commercialization, *Proceedings,* 4th International Conference on Sol Power from Space, Granada, Spain, 2004

Paper submitted: June 13, 2011
Paper revised: July 12, 2011
Paper accepted: September 2, 2011